ACTIVE MICROWAVE IMAGING FOR BREAST CANCER DETECTION

G. Bindu, A. Lonappan, V. Thomas, C. K. Aanandan, and K. T. Mathew

Department of Electronics
Microwave Tomography and Materials Research Laboratory
Cochin University of Science and Technology
Kochi-682 022, India

S. J. Abraham

Department of Surgery
Lourde Hospital
Kochi, India

Abstract—Active microwave imaging is explored as an imaging modality for early detection of breast cancer. When exposed to microwaves, breast tumor exhibits electrical properties that are significantly different from that of healthy breast tissues. The two approaches of active microwave imaging — confocal microwave technique with measured reflected signals and microwave tomographic imaging with measured scattered signals are addressed here. Normal and malignant breast tissue samples of same person are subjected to study within 30 minutes of mastectomy. Corn syrup is used as coupling medium, as its dielectric parameters show good match with that of the normal breast tissue samples. As bandwidth of the transmitter is an important aspect in the time domain confocal microwave imaging approach, wideband bowtie antenna having 2:1 VSWR bandwidth of 46% is designed for the transmission and reception of microwave signals. Same antenna is used for microwave tomographic imaging too at the frequency of 3000 MHz. Experimentally obtained time domain results are substantiated by finite difference time domain (FDTD) analysis. 2-D tomographic images are reconstructed with the collected scattered data using distorted Born iterative method. Variations of dielectric permittivity in breast samples are distinguishable from the obtained permittivity profiles.

1. INTRODUCTION

Breast cancer affects many women and early detection aids in fast and effective treatment. X-ray mammography is currently the most effective imaging method for detecting clinically occult breast cancer. However, despite significant progress in improving mammographic techniques for detecting and characterizing breast lesions, mammography reported high false-negative rates [1] and high false-positive rates [2]. These difficulties are attributed to the intrinsic contrast between normal and malignant tissues at X-ray frequencies. In X-ray tomography a tissue is differentiated based on density. However in most cases, tissue density does not depend on tissue physiological state. Important tissue characteristics such as temperature, blood content, blood oxygenation and ischemia cannot be differentiated by X-ray tomography. For soft tissues like human breast, X-ray cannot image the breast anomalies at an early stage, as there is no significant variation in density between normal and malignant breast tissues [3].

Microwave imaging is a new technology which has potential applications in the field of diagnostic medicine [4, 5]. The basic motivation for this is improved physiologic and pathophysiologic correlation, especially in soft tissue. This expectation is based on the molecular (dielectric) rather than atomic (density) based interactions of the microwave radiation with the target when compared with X-ray imagery. When exposed to microwaves, the high water content of malignant breast tissues cause significant microwave scattering than normal fatty breast tissues that have low water content. It is reported that dielectric permittivity and conductivity increase for cancerous breast tissue is three or more times greater than the host tissue [6]. Due to the improved dielectric contrast, better tissue characterization too is possible.

Microwaves can be used effectively for the detection of biological anomalies like tumor at an early curable stage itself. At microwave frequencies the sensitivity, specificity and the ability to detect small tumors is the dielectric contrast between normal and malignant breast tissues [7]. Malignant breast tissues exhibit considerable increase in bound water content compared to the normal tissues and hence a high value of permittivity. When exposed to microwaves, the high water content of malignant breast tissues cause significant microwave scattering than normal fatty breast tissues that have low water content.

Some benign tumors too respond to microwaves similar to that of malignant tumors [8]. However, characterizing and analyzing such benign tumors is not considered in this paper.

Many prototypes of active microwave imaging has been reported

[7, 9]. The need for using suitable coupling medium to enhance the coupling of electromagnetic energy to the object as well as to increase the resolution is emphasized [10]. A suitable coupling medium accomplishes wavelength contraction without propagation loss penalty associated with increased frequency. In near field microwave medical imaging environment, resolution is determined by the aperture dimensions of the antenna, which can be generalized to far field by using a suitable coupling medium. Also bandwidth enhancement in time domain confocal microwave imaging applications is made possible by its usage. A contrast in the dielectric properties of the object and the coupling medium decreases the measurement accuracy, increases the attenuation, creates temperature drifts and unpredictable local temperature gradients [11].

This paper analyzes the two approaches of active microwave imaging — confocal microwave technique with measured reflected signals and microwave tomographic imaging with measured scattered signals.

2. MODELS

2.1. System Configuration

The designed prototype of 2-D microwave imaging is shown in Figure 1. The breast sample supported on a PVC holder is mounted on a circular platform capable of circular motion in the horizontal plane. The platform along with samples is kept inside a tomographic chamber of radius 12 cm and height 30 cm, coated inside with suitable absorbing material. The chamber is filled with coupling medium. Suspended bowtie antennas are used for both transmission and reception of microwave energy. All measurements are done using HP 8510 C network analyzer; interfaced with Compaq work station SP 750 using GPIB bus.

2.2. Coupling Medium

Proper selection of coupling medium is essential for better resolution of the reconstructed images. In [9] conventional coupling medium like water was used for microwave breast imaging. The variations of the tissue contents in the breast, like fat versus normal tissue were sensed here. A cancerous growth was not considered for the study; also, the obtained permittivity values were significantly greater than that of breast tissues reported in [6]. This may be due to the poor coupling of electromagnetic energy in to the breast volume, as water exhibits considerable permittivity contrast with that of the breast tissues. The
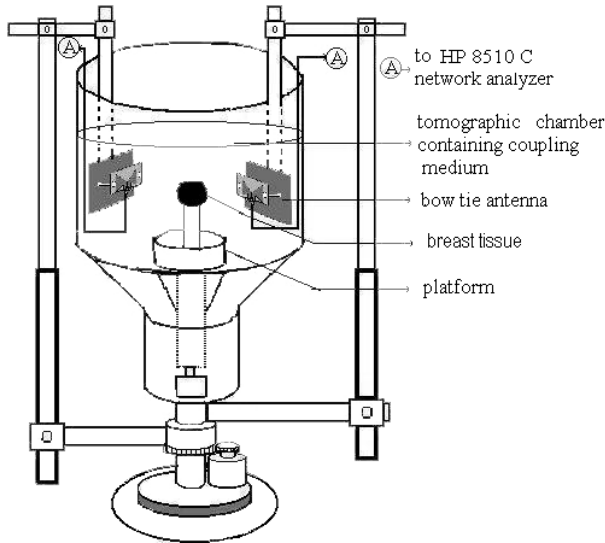
Figure 1. Experimental set up.

higher conductivity of water results in significant propagation losses too.

In the present study the coupling medium used is corn syrup. Dielectric parameters of the material in the frequency range of 2000–4000 MHz are done using cavity perturbation technique [12, 13]. The results are compared with that of the breast tissue data [6] and good agreement is observed [12]. This frequency range is adopted, as the resonant frequency of the antenna used in our microwave imaging studies is 3000 MHz. Also it conveniently includes the Industrial Scientific and Medical (ISM) applications band of 2450 MHz. The dielectric permittivity and conductivity variations of corn syrup in the frequency range of 2000–4000 MHz are shown in Figure 2. It is observed that for corn syrup, the dielectric permittivity decreases and conductivity increases, with the increase in frequency. This result coincides with the studies on dielectric properties of biological tissues [14].

The complex permittivity of the medium can be written as

$$\varepsilon_r = \varepsilon_r' - j\varepsilon_r'' \tag{1}$$

where ε_r' is the dielectric permittivity and ε_r'' is the dielectric loss of the medium. The loss tangent

$$\tan\delta = \varepsilon_r''/\varepsilon_r' \tag{2}$$
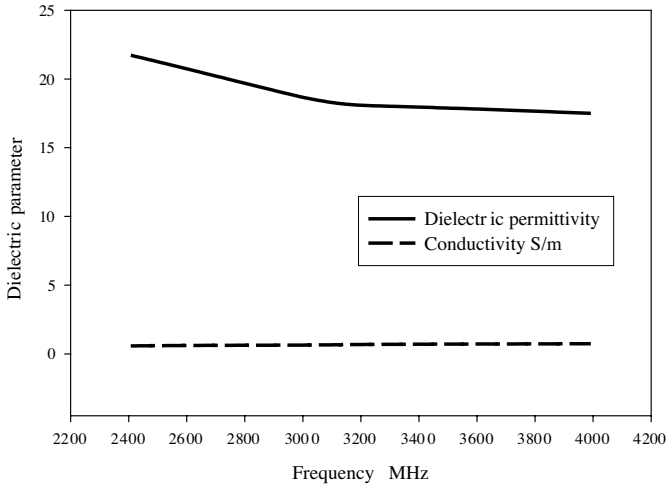
Figure 2. Variation of dielectric permittivity and conductivity for corn syrup.

The propagation constant

$$\gamma = \sqrt{j\omega\mu_0(\sigma + j\omega\varepsilon)} = \alpha + j\beta \tag{3}$$

where α represents the attenuation factor and β the phase factor. The conductivity σ is given by

$$\sigma = \omega\varepsilon_0\varepsilon_r'' \tag{4}$$

Substituting Equations (1), (2) and (4) in (3) and simplifying, we get

$$\alpha = 2\pi f \sqrt{\mu_0\varepsilon_0\varepsilon_r' \left[\sqrt{1 + \tan^2\delta} - 1\right]} \tag{5}$$

and

$$\beta = 2\pi f \sqrt{\mu_0\varepsilon_0\varepsilon_r' \left[\sqrt{1 + \tan^2\delta} + 1\right]} \tag{6}$$

If the wave is considered traveling in the $+z$ direction, $e^{-\alpha z}$ represents the decaying envelope of the wave and $e^{-\beta z}$ represents the sinusoidal nature of the wave whose phase is βz. The total loss encountered by the wave over a distance z consists of dissipation loss L_{diss} due to conduction currents being excited in the medium and diffusion loss L_{diff} due to the spherical spreading of energy [11].

They are given by,

$$L_{diss} = 20 \log_{10} e^{\alpha z} \tag{7}$$
$$L_{diff} = 20 \log_{10}(\beta z) - 29.14(dB) \tag{8}$$

Hence the total loss
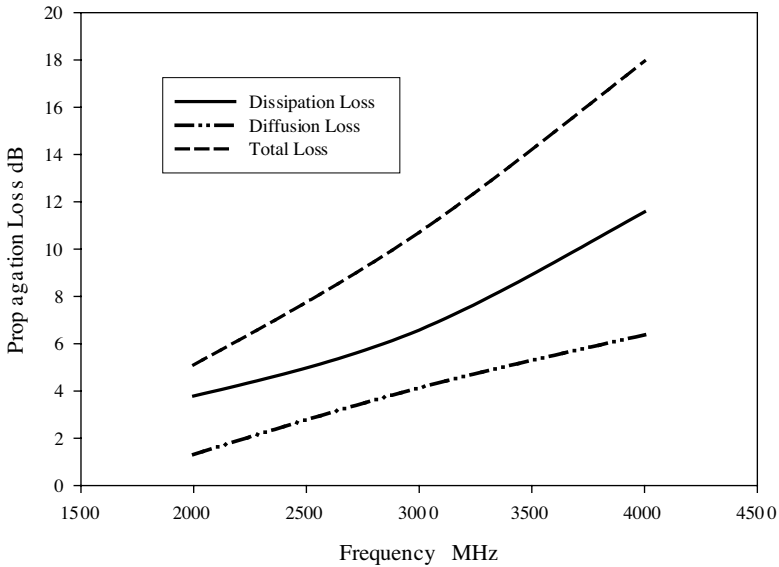
$$L_{total} = L_{diss} + L_{diff} \tag{9}$$

Figure 3. Propagation loss characteristics of corn syrup.

Figure 3 shows the propagation loss characteristics of corn syrup. It is seen that losses increase with frequency, which is due to the increase of conductivity. Table 1 compares the loss parameters of distilled water and saline [11] with corn syrup at 3000 MHz, at a distance of 12 cm. from the transmitter. The loss values are acceptable when compared to the loss parameters of conventional coupling medium like distilled water and saline [11]. It is reported that in water the rate of increase of loss vs. distance is much higher due to the dominant dissipation loss.

2.3. Antenna Design

Coplanar strip line fed bowtie antennas generating TM_{01} mode are designed for both transmission and reception of microwave signals.

Table 1. Propagation loss parameters of water, corn syrup and saline at 3000 MHz at a distance of 12 cm. from the transmitter.

Sample	Total loss dB Dissipation Loss + Diffusion Loss
Corn syrup	10.7
Water	180
Saline (0.5% NaCl)	165

As confocal microwave technique (CMT) is a time domain approach, bandwidth is the major deciding factor in the antenna design. The experimental investigation [15, 16] shows that the designed antenna, in air, exhibits enhanced 2:1 VSWR bandwidth of ∼46% in the operational band of 1850–3425 MHz with a return loss of −53 dB. In corn syrup, the bandwidth is enhanced to 91% in the range of 1215 MHz–3810 MHz with resonant frequency of 2855 MHz and return loss of −41 dB. Figure 4 shows the radiation characteristics of the antenna. This enhanced bandwidth is beneficial to transmit short transient pulses in CMT. The same antenna is used for microwave tomographic imaging too at the frequency of 3000 MHz.
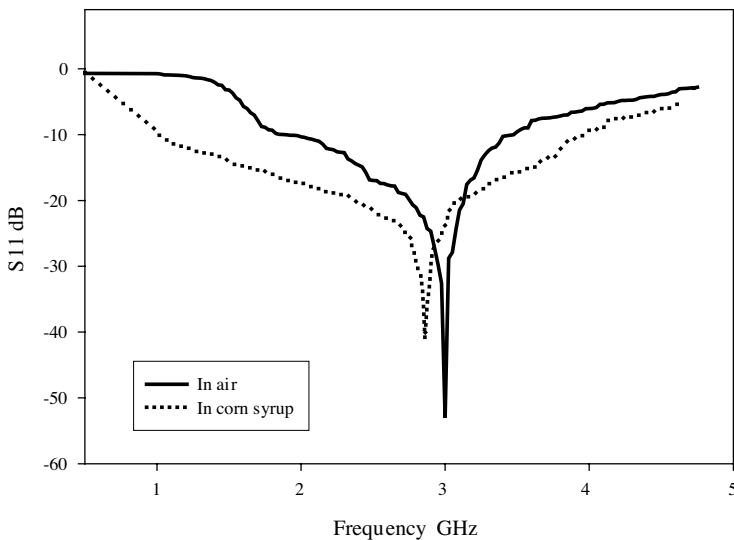

Figure 4. Radiation characteristics of bowtie antenna.

2.4. Samples

Samples of breast tissues of four patients are collected from Department of Surgery, Lourde Hospital, Kochi and are subjected to study within 30 minutes of mastectomy. Cancerous tissue of $\sim$ radius 0.5 cm inserted in normal tissue of $\sim$ radius 1 cm, of patient 1, is taken as sample 1. Samples 2 and 3 consists of four tumorous inclusions of $\sim$ radius 0.25 cm each inserted in normal tissue of $\sim$ radius 1 cm, of patients 2 and 3. Scattered inclusions of cancerous tissue of $\sim$ radius 0.1 cm each inserted in normal tissue, of patient 4 is treated as sample 4. The samples are supported on a cylindrical PVC holder ($\tan \delta = 0.0018$ and $\varepsilon_r = 2.4$ at 3000 MHz) of height 15 cm at the center of the measurement set up as shown in Figure 1.

3. METHODS

3.1. Confocal Microwave Technique

Versions of video pulse radars were first introduced for medical applications as a means to detect malignancy in internal biological tissues by Hagness et al. [17, 18]. Fear et al. [5, 19, 20] demonstrated the feasibility of detecting and localizing small tumors in three dimensions. In contrast to X-ray mammography, the non-ionizing CMT exploits the translucent nature of the breast and obtains a large dielectric contrast of the tissues according to their water content. Moreover CMT avoids complex image reconstruction algorithms. As the illuminating signal is wide band, a simple time shifting and summing the signals are enough to detect the malignant tissues.

3.1.1. Data Acquisition

In CMT, same antenna is used for both transmission and reception of microwave energy. To acquire data, the tissue sample is illuminated by the wide band bowtie antenna and the same antenna collects the back-scattered waves. The antenna is rotated around the sample at a radius of 6 cm and measurements are taken for every $10°$ position of the antenna. A time-shift-and-add algorithm is applied to the set of recorded pulses to enhance the returns from high contrast regions and reduce clutter. This involves computing the time delay for the roundtrip between each antenna position to a point in the domain of interest, then adding the corresponding portions of the time signals recorded at each antenna position.

3.1.2. FDTD Analysis

To validate the experimental investigation, the theoretical analysis is done using finite difference time domain (FDTD) method. The dispersive nature of the dielectric medium is incorporated in the constitutive FDTD equations using first order Debye dispersion relation [21, 22]. The geometry under consideration consists of an infinitely long multilayered cylinder of dispersive dielectric nature with its axis in the z direction. In the z direction the scatterer geometry is assumed to be uniform, and hence the field variations are zero. When this assumption is incorporated in the Maxwell's curl equations, the variations of the electric and magnetic fields exist only with respect to the x and y spatial coordinate variables and with respect to the time parameter variable. For the source excitation a constant current source confined in the xz plane polarized in the negative z direction is considered. So the x and y components of the electric current density do not exist. Hence the problem is treated as 2-D with only E_z, H_x, and H_y fields present. The electric and magnetic fields in a non magnetic medium is given by,

$$H_x(i, j, t+1) = H_x(i, j, t) - \frac{dt}{\mu_0 dy}(E_z(i, j, t) - E_z(i, j-1, t)) \quad (10)$$

$$H_y(i, j, t+1) = H_y(i, j, t) - \frac{dt}{\mu_0 dx}(E_z(i, j, t) - E_z(i-1, j, t)) \quad (11)$$

$$E_z(i, j, t+1) = \frac{\varepsilon_\infty}{\varepsilon_\infty + \chi_0(i, j)} E_z(i, j, t)$$

$$+ \frac{1}{\varepsilon_\infty + \chi_0(i, j)} \sum_{m=0}^{t-1} E_z(i, j, t-m)\Delta\chi_m(i, j)$$

$$+ \frac{dt}{\varepsilon_\infty + \chi_0(i, j)\varepsilon_0 dx}(H_y(i+1, j, t) - H_y(i, j, t))$$

$$- \frac{dt}{\varepsilon_\infty + \chi_0(i, j)\varepsilon_0 dy}(H_x(i, j+1, t) - H_x(i, j, t))$$

$$(12)$$

where

$$\chi_0(i, j) = (\varepsilon_s - \varepsilon_\infty)(1 - \exp(-dt/t_0)) \quad (13)$$

is the susceptibility function.

$$\Delta\chi_m(i, j) = (\varepsilon_s - \varepsilon_\infty)(\exp(-mdt/t_0)(1 - \exp(-dt/t_0))^2 \quad (14)$$

where ε_s is the static permittivity, ε_∞ is optical permittivity and t_0 is the dielectric relaxation time. A Gaussian pulse of half width T as 18 ps

with time delay of 54 ps is selected as the source of excitation. The computational domain is discretized as 120×120 Yee cells. Space step of 1 mm and time step of 6.05 ps are chosen to ensure propagation of the waves in the entire domain. Mur's second order absorbing boundary conditions are applied to terminate the FDTD grid.

3.2. 2-D Microwave Tomographic Imaging

The problem of microwave tomographic imaging has been a topic of theoretical and experimental study for many years. Several research groups are investigating microwave tomography for breast cancer detection [23–26].

3.2.1. Data Acquisition

For data acquisition, the breast sample is illuminated by bow-tie antenna at a frequency of 3000 MHz. As shown in Figure 1, the transmitting antenna is fixed at a radius of 6 cm. on the circular rail, while the receiving antenna is rotated around the object at 6 cm. radius. The platform upon which the sample is mounted is rotated from 0° to 360° in steps of 10° and the receiving antenna is rotated from 30° to 330° in steps of 10°. For every 10° rotation of the platform with the sample, the receiving antenna makes the measurement in steps of 10°.

3.2.2. Reconstruction Algorithm

The contrast in the dielectric properties of the object creates multiple scattering of the wave inside the object. This poses a non linear inverse scattering problem which is formulated in terms of Fredholm integral equation of the second kind [27]. The object is considered inhomogeneous in the xy plane but homogeneous in the z direction. For an incident TM wave, the total electric field at the receiver [28] is given by,

$$\phi(r) = \phi_{inc,b}(r) + \omega^2 \mu \int_S dS g_b(r, r') \delta\varepsilon(r')\phi(r') \tag{15}$$

where r stands for a point in the measurement domain and r' for the object domain. $\phi_{inc, b}(r)$ is the incident field in the presence of the background inhomogeneity and the integral term is the scattered field due to the dielectric contrast between the scatterer and the background medium.

$$\delta\varepsilon(r') = \varepsilon(r') - \varepsilon_b(r') \tag{16}$$

is called as the object function, the Green's function and $g_b(r, r')$ the total electric field inside the scatterer. Equation (15) is used for both the forward and inverse solutions. In the forward problem, both the medium properties and the domain of inhomogeneity are known and the equation is solved to obtain the total electric field. In the inverse problem, scattered fields are measured at discrete points and the medium properties are the unknowns to be determined. The problem is linearized using distorted Born approximation [28] by replacing $\phi(r')$ with $\phi_{inc,b}(r)$. As the background medium is inhomogeneous, Green's function is solved numerically [29]. Discretization of the integral equation in the inverse problem yields vector representations of the scattered field and the object profile. As the inverse problem is ill posed, a regularization procedure [27, 28] is employed where an optimization technique is adopted to minimize the error by minimizing a cost functional. The non-uniqueness and instability of the problem is thus circumvented and an adequate solution is provided. The obtained $\delta\varepsilon$ is used to improve $\varepsilon_b(r)$ which in turn is used to update the parameters in Equation (15). The iteration is continued until convergence is reached. The imaging area is restricted to 16×16 pixels due to computational complexity. The sampling rate considered is 0.1λ.

4. RESULTS AND DISCUSSIONS

Corn syrup sample of dielectric permittivity and conductivity as 18.7 and $0.64\,\text{S/m}$ at 3000 MHz is used as the coupling medium in this study. In order to check the compatibility of corn syrup with breast tissue samples, dielectric properties of the breast tissue samples are measured using cavity perturbation technique and are compared with that of the corn syrup at a frequency of 3000 MHz. Table 2 shows the comparison. The measured dielectric parameters of breast tissues match with the literature data too [6, 30]. When corn syrup is used as coupling medium for imaging normal breast tissue with cancerous inclusion, good resolution is achieved as the dielectric permittivity of corn syrup matches with that of the normal breast tissue as seen in Table 2. As the conductivity of the medium is less than that of the actual tissue sample, loss tangent decreases and hence the propagation loss.

Figures 5–8 show the time domain response of the breast tissue samples 1–4. In all the figures, the first and the last peaks in the encircled region, represent reflections from the corn syrup — normal tissue interface. As the dielectric contrast is less here, the reflections are less compared to the reflections produced by the cancerous

Table 2. Dielectric parameters of breast tissue samples and corn syrup measured using cavity perturbation technique at 3000 MHz.

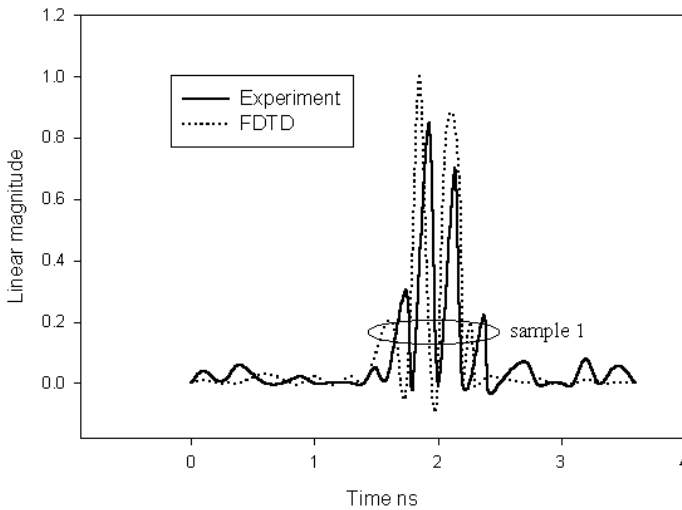| Sample		Dielectric permittivity	Conductivity S/m
Breast tissue, Patient 1	Normal	24.82	1.21
	Cancerous	32.31	1.95
Breast tissue, Patient 2	Normal	18.85	0.72
	Cancerous	38.73	2.25
Breast tissue, Patient 3	Normal	19.98	0.92
	Cancerous	39.5	2.33
Breast tissue, Patient 4	Normal	23.7	1.15
	Cancerous	29.2	1.37
Corn syrup		18.7	0.64

Figure 5. Time domain responses of sample 1 (of patient 1) — single cancerous tissue of ∼ radius 0.5 cm inserted in normal tissue of ∼ radius 1 cm.
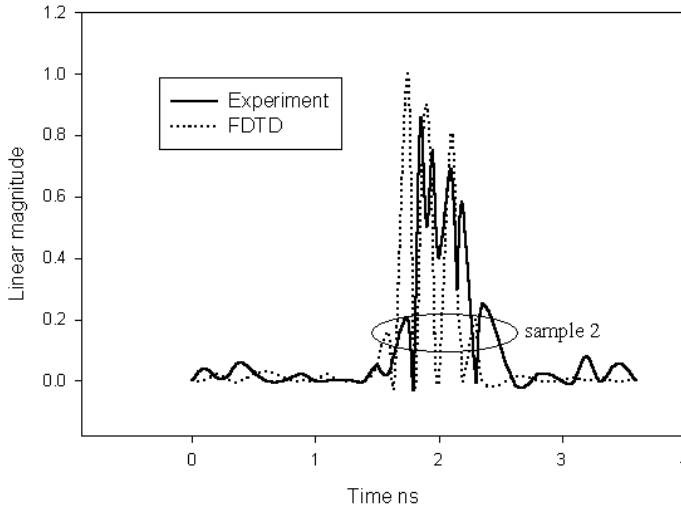
Figure 6. Time domain responses of sample 2 (of patient 2) — four tumorous inclusions of $\sim$ radius 0.25 cm each, inserted in normal tissue of $\sim$ radius 1 cm.

tissues. Other tall peaks correspond to the reflections from the tumor inclusions. In Figure 5, experimental and FDTD results show good agreement as there is only a single tumour inclusion in sample 1. The FDTD and experimental results do not agree well in Figures 6–8, due to the presence of multiple inclusions. Reflections from nearby contrast points overlap and get represented as a single point. The time shift and add algorithm applied to the experimental data makes the reflected signals from tumors located opposite to each other to overlap. Even though exact tumor locations are difficult to figurize, regions of dielectric contrast are satisfactorily detected using this time domain confocal microwave technique. Approximate tumor locations with respect to the tallest peak in the figures are calculated from the equation for velocity of propagation.

The velocity of propagation depends on the dielectric permittivity of the medium given by,

$$\nu = \frac{2d}{t} \tag{17}$$

where

$$\nu = \frac{c}{\sqrt{\varepsilon_r}} \tag{18}$$

d is the distance, t is the time taken for propagation, ε_r is the dielectric constant of the medium/normal tissue measured using cavity
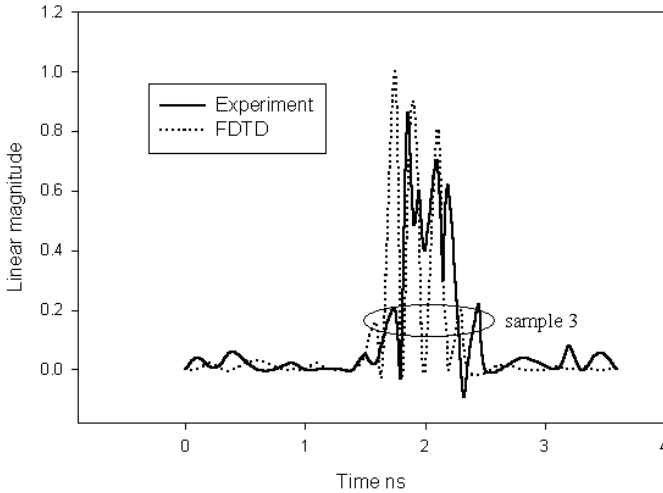
Figure 7. Time domain responses of sample 3 (of patient 3) — four tumorous inclusions of ∼ radius 0.25 cm each, inserted in normal tissue of ∼ radius 1 cm.

perturbation technique and c is the velocity of light in free space. The results are tabulated in Table 3.

The reconstructed 2-D tomographic images for the breast samples 1–4 are shown in Figures 9–12. The dielectric contrast of the samples is clearly distinguishable from the images as well as from the permittivity profiles. Samples 1–3 are having ∼ circular cross section without any cover, where as sample 4 is covered in a thin conical polythene paper. This is done to check whether the shape of the sample too is

Table 3. Approximate tumor locations with respect to the first tumorous inclusion (i.e., with respect to the tallest peak in time domain graphs).

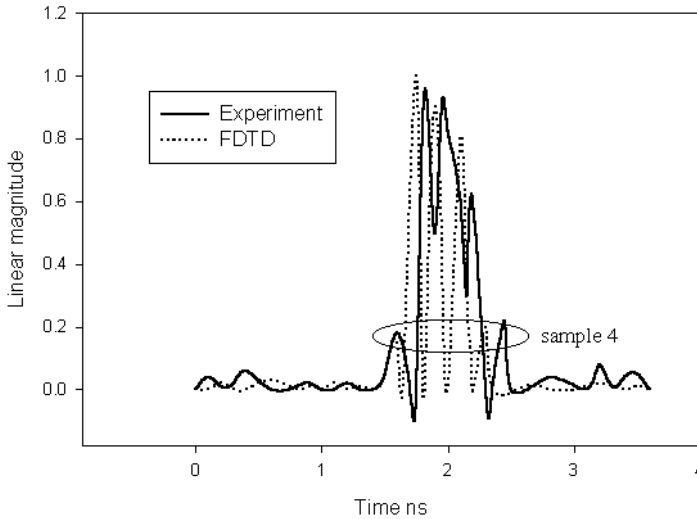| Sample	Actual distance of tumor from the antenna (cm)	Approximate distance calculated from experimental time domain data (cm)
1	7	6.38
2	6.5	6.16
3	6.5	6.06
4	6.5	6.1

Figure 8. Time domain responses of sample 4 (of patient 4) — scattered tumorous inclusions of ∼ radii 0.1 cm. each inserted in normal tissue.

reconstructed properly. As the dielectric permittivity of the coupling medium and the normal breast tissue samples are in good match, the tumor inclusions are clearly visible in Figures 9–11. In Figure 12, the shape of the sample too is reconstructed and is seen with a black border. This is due to the fact that polythene paper exhibits a very low permittivity of ε_r 2.2 at 3000 MHz. Scattered tumor inclusions are clearly distinguishable in the image. A resolution of 2 mm is achieved in this reconstruction with the use of corn syrup as the coupling medium. A comparison of the obtained permittivity values of the breast samples from Figures 9–12 with that measured using cavity perturbation technique reported in Table 2 shows good agreement.

5. SOURCES OF ERROR AND ACCURACY CONDITIONS

Early stage tumor detection is the attractive feature of the proposed microwave medical imaging. So care is taken to eliminate all possible types of errors. In the present study HP 8510 network analyzer is used. Accuracy of this instrument is 0.001 dB for power measurement, 1 Hz for frequency measurement and 0.01 ns for time domain measurement [31]. Main sources of experimental errors are 1) Edge reflections from
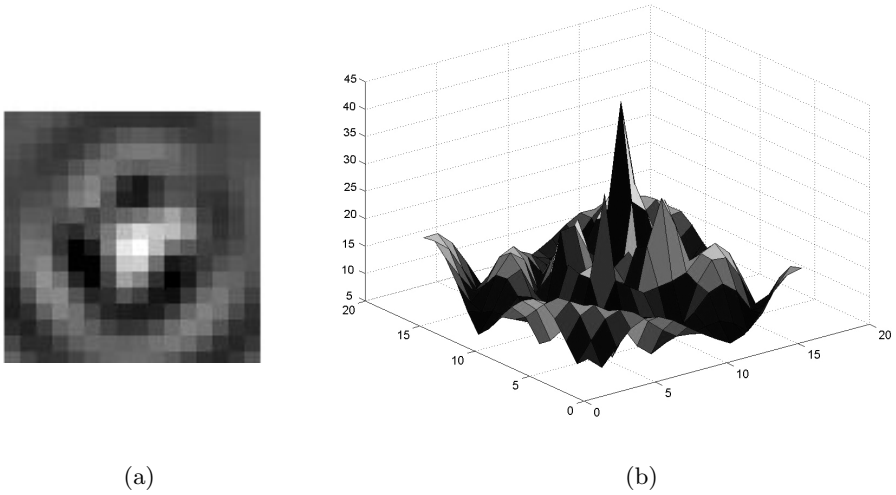
(a)   (b)

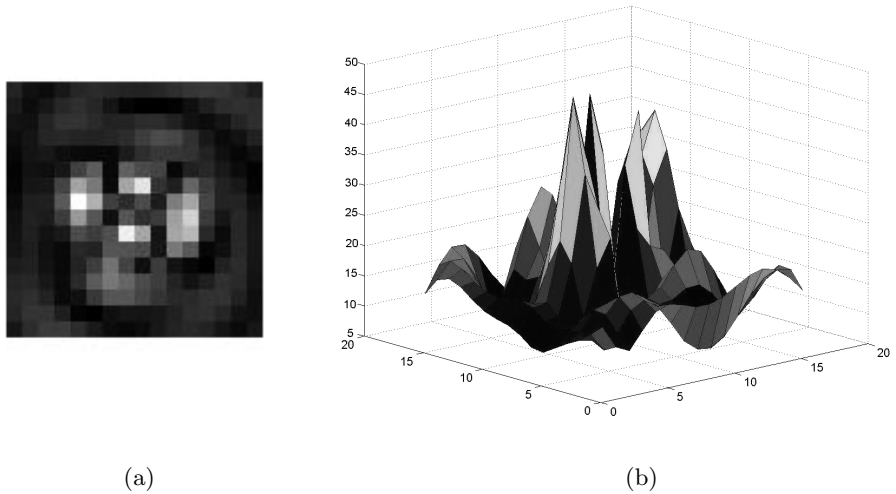**Figure 9.** Sample 1 — a) 2 D microwave tomographic image. b) Dielectric permittivity profile.

(a)   (b)

Figure 10. Sample 2 — a) 2 D microwave tomographic image. b) Dielectric permittivity profile.

(a)   (b)

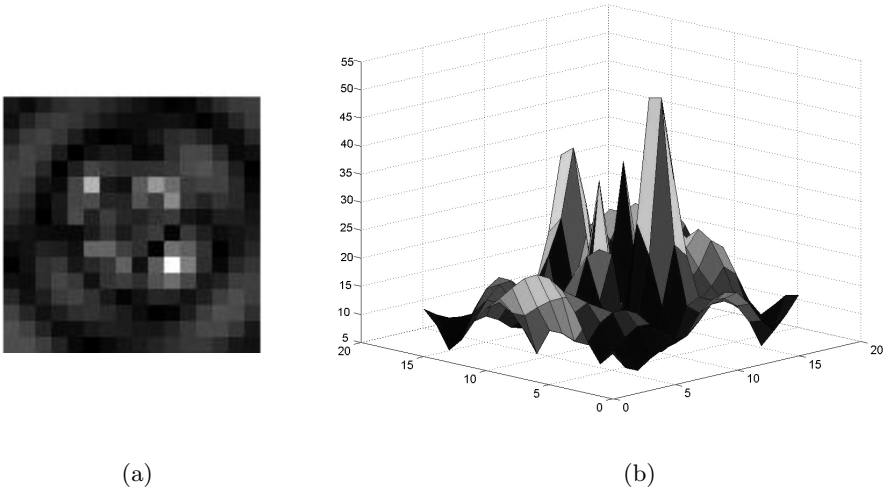**Figure 11.** Sample 3 — a) 2 D microwave tomographic image. b) Dielectric permittivity profile.

(a)   (b)
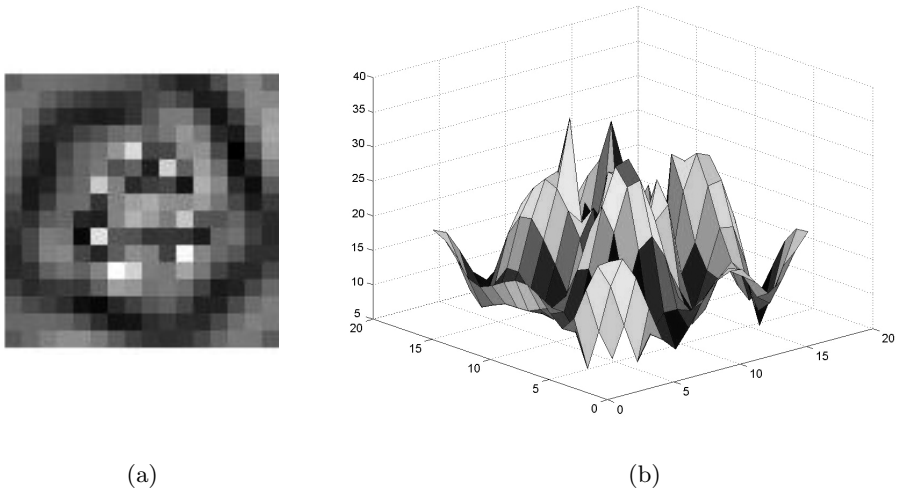
Figure 12. Sample 4 — a) 2 D microwave tomographic image. b) Dielectric permittivity profile.

the antenna: The FDTD computed end-reflections observed at the feed point of the bowtie antenna relative to the exciting pulse is -24 dB. For the CMT a time gating of 9.07 ns is provided from the network analyzer to remove these reflections. More over calibration of the system was performed in the coupling medium in the absence of the breast samples. 2) Reflections from the sample holder: The tissue samples are supported on a low loss PVC pipe having loss tangent ($\tan \delta$) 0.002. Hence reflections are negligible. 3) Medium reflections: As the tumor under study is immersed in a matching coupling medium, reflections are minimized and good resolution of the reconstructed image is ensured. 4) Validity of distorted Born approximation to linearize the inverse scattering problem: This method is adopted to reduce the computational complexity. Acceptable values of permittivity profiles are obtained with in vitro breast studies. The matter has to be further investigated with strong scatterers and fast forward iterative solvers. 5) Convergence: To ensure that global convergence is achieved, we performed five iterations and the same profile as with the fourth iteration was obtained.

6. CONCLUSION

Active microwave imaging is explored as an imaging modality for early detection of breast cancer. In vitro studies on normal and malignant breast tissues suggest that microwave tomographic imaging could satisfactorily image the tissues showing clear discrimination in terms of dielectric permittivity. Using confocal microwave technique, the location of the tumor could be satisfactorily detected as the strength of the reflected signals in the time domain varies with dielectric contrast which in turn depend on the bound water content of the tissues. Hence microwave imaging can be considered for early stage breast cancer detection.

REFERENCES

1. Huynh, P. T., A. M. Jarolimek, and S. Dayee, "The false-negative mammogram," *Radiographics*, Vol. 18, 1137–1154, 1998.

2. Elmore, J. G., M. B. Barton, V. M. Moceri, S. Polk, P. J. Arena, and S. W. Fletcher, "Ten year risk of false positive screening mammography and clinical breast examinations," *New England Journal of Medicine*, Vol. 338, 1089–1096, 1998.

3. Fear, E. C. and M. A. Stuchly, "Microwave detection of breast cancer," *IEEE Transactions on Microwave Theory and Techniques*, Vol. 48, 1854–1863, 2000.

4. Fear, E. C., S. C. Hagness, P. M. Meaney, M. Okoniewski, and M. A. Stuchly, "Enhancing breast tumor detection with near field imaging," *IEEE Microwave magazine*, Vol. 3, 48–56, 2002.

5. Fear, E. C., X. Lii, S. C. Hagness, and M. A. Stuchly, "Confocal microwave imaging for breast cancer detection: localization of tumors in three dimensions," *IEEE Transactions on Biomedical Engineering*, Vol. 49, 812–821, 2002.

6. Chaudhary, S. S., R. K. Mishra, A. Swarup, and J. M. Thomas, "Dielectric properties of normal and malignant human breast tissues at radiowave and microwave frequencies," *Indian Journal of Biochemistry and Biophysics*, Vol. 21, 76–79, 1981.

7. Semenov, S. Y. et al., "Microwave tomography: Two-dimensional system for biological imaging," *IEEE Transactions on Biomedical Engineering*, Vol. 43, 869–877, 1996.

8. Rangayyan, R. M., N. M. El-Faramawy, J. E. L. Desautels, and O. A. Alim, "Measures of acutance and shape for classification of breast tumor," *IEEE Transactions on Medical Imaging*, Vol. 16, 799- 810, 1997.

9. Meaney, P. M., M. W. Fanning, D. Li, S. P. Poplack, and K. D. Paulsen, "A clinical prototype of active microwave imaging of the breast," *IEEE Transactions on Microwave Theory and Techniques*, Vol. 48, 1841–1853, 2000.

10. Meaney, P. M., S. A. Pendergrass, M. W. Fanning, D. Li, and K. D. Paulsen, "Importance of using reduced contrast coupling medium in 2D microwave breast imaging," *Journal of Electromagnetic Waves and Application*, Vol. 17, 333–355, 2003.

11. Foti, S. J., R. P. Flam, J. F. Aubin, L. E. Larsen, and J. H. Jacobi, "A water immersed microwave phased array system for interrogation of biological targets," *Medical Applications of Microwave Imaging*, 148–166, IEEE Press, New York, 1986.

12. Bindu, G., A. Lonappan, V. Thomas, V. Hamsakutty, C. K. Aanandan, and K. T. Mathew, "Microwave characterization of breast phantom materials," *Microwave and Optical Technology Letters*, Vol. 43, 506–508, 2004.

13. Mathew, K. T. and U. Raveendranath, *Sensors Update*, 185–210, Wiley–VCH, Germany, 1999.

14. Gabriel, S., R. W. Lau, and C. Gabriel, "Dielectric properties of biological tissues: II. Measurements in the frequency range 10 Hz to 20 GHz," *Physics in Medicine and Biology*, Vol. 41, 2251–2269, 1996.

15. Bindu, G. et al., "Wideband bowtie antenna with coplanar stripline feed," *Microwave and Optical Technology Letters*, Vol. 42, 222–224, 2004.

16. Bindu, G., A. Lonappan, C. K. Aanandan, and K. T. Mathew, "Wideband bowtie antenna for confocal microwave imaging," *Asia Pacific Microwave Conference 2004*, APMC 04/C/449, New Delhi, India, 2004.

17. Hagness, S. C., A. Taflove, and J. E. Brdiges, "Two-dimensional FDTD analysis of a pulsed microwave confocal system for breast cancer detection: fixed focus and antenna array sensors," *IEEE Transactions of Biomedical Engineering*, Vol. 45, 1470–1479, 1998.

18. Hagness, S. C., A. Taflove, and J. E. Brdiges, "Three-dimensional FDTD analysis of a pulsed microwave confocal system for breast cancer detection: Design of an antenna array element," *IEEE Transactions of Antennas and Propagation*, Vol. 47, 783–791, 1999.

19. Fear, E. C., J. Sill, and M. A. Stuchly, "Experimental feasibility of breast tumor detection and localization," *IEEE MTT-S Digest*, 383–386, 2003.

20. Fear, E. C., J. Sill, and M. A. Stuchly, "Experimental feasibility study of confocal microwave imaging for breast tumor detection," *IEEE Transactions on Microwave Theory and Techniques*, Vol. 51, 887–892, 2003.

21. Kosmas, P., C. M. Rappaport, and E. Bishop, "Modeling with the FDTD method for microwave breast cancer detection," *IEEE Transactions on Microwave Theory and Techniques*, Vol. 52, 1890–1897, 2004.

22. Luebbers, R., F. P. Hunsberger, K. S. Kunz, R. B. Standler, and M. Schneider, "A frequency dependent finite-difference time domain formulation for dispersive materials," *IEEE Transactions on Electromagnetic Compatibility*, Vol. 32, 222–227, 1990.

23. Meaney, P. M., K. D. Paulsen, A. Hartov, and R. K. Crane, "Microwave imaging of tissue assessment: Initial evaluation in multitarget tissue equivalent phantoms," *IEEE Transactions on Biomedical Engineering*, Vol. 43, 878–890, 1996.

24. Li, D., P. M. Meaney, T. Raynolds, S. Pendergrass, M. Fanning, and K. D. Paulsen, "A parallel-detection microwave spectroscopy system for breast imaging," *Review of Scientific Instruments*, Vol. 75, 2305–2313, 2004.

25. Meaney, P. M., K. D. Paulsen, and J. T. Chang, "Near-field microwave imaging of biologically based materials using a monopole transceiver system," *IEEE Transactions on Microwave Theory and Techniques*, Vol. 46, 31–44, 1998.

26. Bulyshev, A. E. et al., "Computational modeling of three-dimensional microwave tomography of breast cancer," *IEEE Transactions on Biomedical Engineering*, Vol. 48, 1053–1056, 2001.

27. Taflove, A., *Advances in Computational Electrodynamics: The Finite Difference Time Domain Method*, Artech House. Inc., Norwood, MA, 1998.

28. Chew, W. C. and Y. M. Wang, "Reconstruction of two-dimensional permittivity distribution using the distorted born iterative method," *IEEE Transactions on Medical Imaging*, Vol. 9, 218–225, 1990.

29. Richmond, J. H., "Scattering by a dielectric cylinder of arbitrary cross section shape," *IEEE Transactions on Antennas and Propagation*, Vol. 13, 334–341, 1965.

30. Campbell, A. M. and D. V. Land, "Dielectric properties of female human breast tissue measured in vitro at 3.2 GHz," *Physics in Medicine and Biology*, Vol. 37, 193–210, 1992.

31. *HP 8510C Network Analyzer Operating and Programming Manual*, Hewlett-Packard, 1988.